



JOURNAL OF THE ACADEMIC SOCIETY FOR QUALITY OF LIFE (JAS4QoL)

2020 VOL. 6(1) 2:1-10

DEVELOPMENT OF A FREE-ELECTRON LASER IN THE TERAHERTZ REGION

Goro ISOYAMA

Institute of Scientific and Industrial Research, Osaka University, 8-1 Mihogaoka, Ibaraki, Osaka 567-0047, Japan
isoyama@sanken.osaka-u.ac.jp

Citation: ISOYAMA, G. Development of a Free-Electron Laser in the Terahertz Region *JAS4QoL* **2020**, 6(1) 2:1-10.

Online: <http://as4qol.org/?p=2894>

Received Date: 2020/11/21 Accepted Date: 2020/11/21 Published: 2020/12/10

ANNOUNCEMENT

- The 2019 International Conference on Quality of Life was held at Kyoto Pharmaceutical University from Sept 28-29, 2019. Further information can be found at <http://as4qol.org/icqol/2019/>
- We have moved to continuous publication. Beginning January 2019 the editing committee has decided to adopt a continuous publishing model for Journal publication. Individual articles will be released online as they become ready, allowing a steady stream of informative quality articles. We will also be moving to a calendar year issue cycle. In traditional terms, each volume will encompass a single year and consist of a single issue. Publishing on a just-in-time basis allows authors to present their results in a timely fashion, and our readers, students, and colleagues to access our content and cite articles more quickly and free from the restrictions of a predefined timetable. As a result of these changes, the look and style, as well as the function, of the Journal will be different, and hopefully improved.
- The 2019 International Meeting on Quality of Life was held recently. Proceedings as well as photos and other information can be found at <http://as4qol.org/icqol/>

MORE INFORMATION AT [HTTP://AS4QOL.ORG/ICQOL/](http://AS4QOL.ORG/ICQOL/)



Development of a Free-Electron Laser in the Terahertz Region

Goro ISOYAMA

¹Institute of Scientific and Industrial Research, Osaka University, 8-1 Mihogaoka, Ibaraki, Osaka 567-0047, Japan (isoyama@sanken.osaka-u.ac.jp)

Abstract

We have been developing a free-electron laser (FEL) in the far-infrared or terahertz (THz) region for higher intensity and stability, using the L-band (1.3 GHz) electron linear accelerator (linac) at the Institute of Scientific and Industrial Research (ISIR), Osaka University. The FEL was progressively upgraded, and the maximum energy of micropulses, which form an FEL macropulse of a duration of some microseconds, reached 260 μJ at a wavelength around 65 μm or a frequency around 4.6 THz, which is an order of magnitude higher than micropulse energies obtained in other FELs in this wavelength or frequency range. Experiments have begun using high-intensity narrow-band terahertz radiation from the FEL. This paper summarized the progress of the FEL and its application experiments.

Keywords: Free Electron Laser (FEL), Electron, Linear Accelerator (Linac), Terahertz (THz), Far-Infrared

1. Introduction

Lasers are one of the greatest inventions of the 20th century since not only they have been contributing to progress in science and technology but they are also widely used in industry, medicine, and our daily lives. A laser stores energy in an excited state of a solid, gas, or liquid, and then generates intense coherent radiation by stimulated emission. Due to characteristics of the excited state, the laser is basically fixed in wavelength, and the operating wavelength is also limited to the infrared, through visible, to ultraviolet regions, with some exceptions.¹ In order to overcome the limitations of conventional lasers, the Free Electron Laser (FEL) was developed and first implemented in 1978 in the infrared region at Stanford University.² Development and utilization of FELs have been extensively conducted throughout the world, as the FEL has potential advantages over other lasers. For example, it can operate in any wavelength region, the wavelength is continuously variable, the output power is high, and the efficiency is also high. In the early stages, mid-infrared FELs based on S-band Radio Frequency (RF) linacs were constructed for various studies since there are many vibrational and rotational states of molecules accessible at those wavelengths.³ To extend the wavelength range, FELs based on electron storage rings were developed, ranging progressively from the infrared, through the visible, to the ultraviolet regions.⁴ Because mirrors for optical cavities are not available beyond the ultraviolet region, single-pass FELs have been developed based on high-energy electron linacs to generate extremely high-intensity coherent X-

Citation: ISOYAMA, G. Development of a Free-Electron Laser in the Terahertz Region. *JAS4QoL* 2020, 6(1) 2:1-10.

Available online at
<http://as4qol.org/?p=2894>

Received: 2020/11/21
Accepted: 2020/11/21
Published: 2020/12/10

©2020 JAS4QoL as4qol.org

rays for crystallography.⁵ High power and high efficiency FELs were also constructed using a superconducting accelerator with an energy recovery system, in which the deteriorated electron beam used for lasing is re-entered into the high efficiency linac and decelerated to transfer its kinetic energy to a newly incoming beam.⁶

The other direction for expanding the wavelength region of FEL is to the longer wavelength or lower frequency region beyond the infrared ray, which is called the far-infrared (FIR) or Terahertz (THz) region. It is located between light and micro waves and is called the terahertz gap because there were originally few strong radiation sources and sensitive detectors for that region. Since the energy of the electron beam is relatively low, various types of electron accelerators are used for THz-FELs, and hence FEL beams with various characteristics are generated and used in experiments.⁷⁻¹²

We began research and development of FEL at the end of 1980s with an L-band electron linac at the Institute of Scientific and Industrial Research (ISIR), Osaka University. In FEL operation, a high peak current or charge in electron bunches and a long electron pulse, which is comprised of many electron bunches, are required: the former to make an FEL gain higher than cavity loss to start lasing and the latter to allow a large number of amplifications for the high power operation to reach power saturation. The first lasing was obtained at wavelengths between 32 and 40 μm in 1994.¹³ In the FEL mode of the linac, the bunch charge was 1 nC, which is higher than that of other S-band linacs for FEL, but the electron pulse length was approximately 2 μs because the first 2 μs part in a 4 μs pulse was lost because of the long filling time of the RF power in the L-band acceleration tube, so that the number of amplifications was limited to only approximately 50 and the FEL could not reach power saturation. As there were few FELs in the far-infrared region at that time, though several infrared FELs were in operation, we suspended development of high power operation and began upgrading the FEL for extending the wavelength region toward longer wavelengths, in which the diffraction loss of radiation stored in the cavity increases and makes it difficult to lase. We progressively remodeled the FEL to expand the aperture of the vacuum ducts in the cavity and succeeded in lasing at a wavelength of 150 μm , which was the longest wavelength at that time obtained in the FELs based on RF linacs.¹⁴

Sometime after the successful operation of the FEL in the long wavelength region, we had an opportunity to upgrade the FEL on the occasion of a large scale renovation of the L-band linac. The target was to realize the high intensity operation of the FEL reaching power saturation, which was expected to be comparable to the micropulse energies of CLIO⁸ and FELIX⁹. In this paper, we introduce our studies on upgrades to the FEL, the L-band linac, and some application experiments of the FEL.

2. FEL at ISIR, Osaka University

2.1 L-band electron linac

Figure 1 shows a schematic diagram of the L-band linac and its beam lines. The L-band linac is opti-

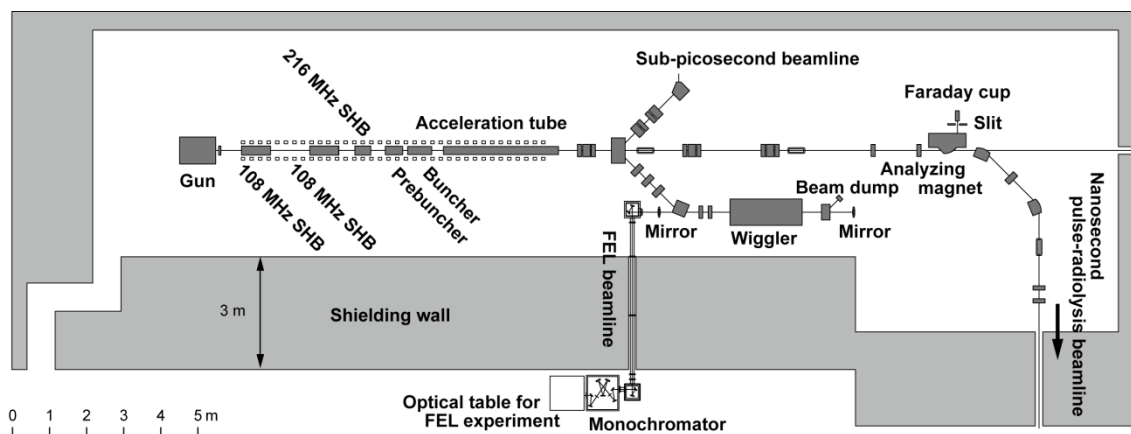


Fig. 1. Schematic drawing of the L-band linac and the FEL system. Electron pulses generated with the electron gun are compressed with the three sub-harmonic bunchers (SHBs), they are captured and compressed in the prebuncher and buncher, and then accelerated in the acceleration tube. The electron beam is bent right and goes through the wiggler, in which it amplifies an FEL pulse or pulses in the optical cavity consisting of two spherical mirrors, and stopped at the beam dump. A fraction of the FEL pulse is taken out through a hole in the upstream mirror and led to the optical table through the evacuated FEL beamline. The grating of the monochromator is replaced with a plane mirror in this experiment.

mized for pulse radiolysis experiments using a high-intensity single-bunch beam. In order to generate such a beam, the linac is equipped with a 100 kV DC electron gun with a large-area thermionic cathode, a three-stage subharmonic buncher system consisting of two 108 MHz RF cavities and one 216 MHz RF cavity, the frequencies of which are respectively 1/12 and 1/6 of the main acceleration frequency of 1.3 GHz in the L-band, followed by a 1.3 GHz pre-buncher, a buncher, and a 3 m long acceleration tube of the travelling wave type.

The L-band linac has been improved several times since its construction in 1979, among which a large-scale upgrade was done in 2003 for higher stability and reproducibility of the linac operation, so that almost all the power supplies and facilities for the linac were replaced except for its RF structures, magnets, and the vacuum system. As a part of this upgrade, a klystron modulator, which is a power supply for a klystron to generate the 1.3 GHz RF power for the linac, was renewed and a new operation mode with pulse duration 8 μ s was added to the modulator for FEL in addition to the conventional 4 μ s pulse mode. As the first 2 μ s portion of the electron pulse is scraped off in the beam transport line to the FEL owing the 2 μ s filling time of the RF power in the acceleration tube, an electron pulse for the FEL was 2 μ s long in the former conventional mode, whereas it is 6 μ s long in the new mode, which is three times longer than the pulse length in the conventional mode.

2.2 FEL system

In general, an FEL consists of an electron accelerator, a wiggler for electrons to radiate monochromatic light, and an optical cavity to amplify stored FEL pulses repeatedly by electron bunches.¹⁵ The wavelength λ of the FEL is given by

$$\lambda = \frac{\lambda_w}{2\gamma^2} (1 + K_{rms}^2), \quad (1)$$

where λ_w is the period length of the wiggler, $\gamma = (E + m_0c^2)/m_0c^2$ is the total energy of an electron in units of its rest mass m_0c^2 with E the kinetic energy of an electron, m_0 its rest mass, and c the speed of light, and K_{rms} is the root-mean-square deflection parameter defined as $K_{rms} = 66 \times \lambda_w [\text{m}] \times B_0 [\text{T}]$ with B_0 the peak magnetic field. A small portion of the FEL pulses in the cavity is extracted via an output coupler, which is usually a through-hole in a mirror for the cavity, and the extracted pulse is called a micropulse and a series of micropulses forms a macropulse.

Table 1 lists the main parameters of the FEL system. The wiggler is the Halbach-type wiggler made only of permanent magnets with a period length $\lambda_w = 6$ cm and the number of periods 32, and its length is 1.938 m, including the magnet blocks for end corrections. The minimum magnet gap is $g = 30$ mm and the peak magnetic field there is $B_0 = 0.37$ T, so that the K_{rms} -value is 1.47. The peak magnetic field B_0 decreases exponentially with increasing wiggler gap. The optical cavity is a 5.531-m-long near-concentric resonator using two spherical mirrors with a diameter of 8 cm made of copper coated with gold, and

Table 1. Main parameters of the FEL system.

Wiggler	Halbach-type planer wiggler
Magnet length, including end corrections	1.938 m
Period length	60 mm
Number of periods	32
Magnet gap	30 - 120 mm
Peak magnetic field	0.37 T
K-value (rms)	0.01 - 1.47
Optical cavity	Near-concentric resonator
Length	5.531 m
Mirrors	Spherical concave mirrors
Diameter	80 mm
Curvature radius : upstream	3358 mm
: downstream	2877 mm
Rayleigh length	1 m at the center of the wiggler
Output coupling	A hole 3 mm in diameter at the center of the upstream mirror

the waist of the stored radiation is located at the center of the wiggler, where the Rayleigh range of the cavity is 1 m. There are a 3-mm-in-diameter through-hole at the center of the upstream mirror to extract a portion of a stored FEL pulse or pulses and a 1-mm-in-diameter through-hole at the center of the downstream mirror to inject a He-Ne laser beam for alignment of instruments at the experimental station. The THz FEL beam extracted from the cavity goes through a 0.2-mm-thick 20-mm-in-diameter polycrystalline diamond window, which transmits the THz beam well, into the transport line of a low vacuum. The FEL beam is transported from the FEL in the accelerator room through a 3-m-thick concrete wall for radiation shielding to the measurement room, and taken out to an experimental table in the air through another diamond window of the same type attached to an evacuated grating monochromator with a plane mirror in place of a diffraction grating, which is located at the end of the FEL transport line.

3. Development of the FEL

After the large-scale refurbishment, the commissioning of the L-band linac went smoothly for pulse radiolysis experiments, whereas recommissioning of the FEL did not work well. The variations of the 1.3 GHz RF power and its phase were found to be larger than 10% and some tens of degrees, respectively, in the RF pulse of width 8 μ s generated by the klystron, but their waveforms did not change for each pulse. As a countermeasure, we have developed a feed forward control with the overdrive technique, which corrects the input RF signal and cancels the output RF power and phase variations, taking into account the slow response of the system.¹⁶ As a result, the RF power and the phase variations were successfully reduced to 0.4% and 0.3 degrees, respectively. The FEL was operated in this new mode, so that the power saturation of the FEL was obtained for the first time.¹⁶ The maximum macropulse energy reached 3.7 mJ at a wavelength of 67 μ m or a frequency of 4.5 THz for an electron beam energy of 18 MeV. The number of micropulses was calculated to be approximately 330 using a macropulse width of approximately 3 μ s and the micropulse intervals of 9.2 ns. The micropulse energy of the FEL is calculated to be approximately 11 μ J using the macropulse energy and the number of micropulses, which is comparable to the micropulse energies of CLIO⁸ and FELIX⁹.

Important requirements for the FEL beam in an experiment are not only its intensity, but also its stability. Because FEL pulses in the cavity are repeatedly amplified and grow exponentially to saturation power, approximately seven orders of magnitude, both macropulse and micropulse energies are heavily influenced by small fluctuations of the electron beam induced by the 1.3 GHz RF power and its phase variations. The feedforward control reduces repeated variations in the RF power and phase, but pulse-to-pulse fluctuations remain. The fluctuations in the RF output from the klystron are due to a thyatron, which is a gas-filled tube and works as a kind of discharge tube. It is used as a high-voltage and high-current switch in the klystron modulator, which provides such pulses to the klystron. Because alternatives to the thyatron are not currently available on the market, we have developed a fast, high-current, and high-voltage switch using solid state devices. The thyatron used in the klystron modulator operates at a holding voltage of 25 kV, a current of 6 kA, a pulse width of 10 μ s, and a repetition rate of 10 Hz, at maximum. We adopted static induction thyristors (SI thyristors) as semiconductor devices for the solid state switch that meets the specifications for the thyatron. The specifications of the SI thyristor are a holding voltage of 2 kV and a peak current of 1 kA. To meet the specifications of the switch, the circuit was configured to be six parallel lines of 10 serially connected thyristors, which were attached, together with their control circuit boards, on the outer walls of six rectangular aluminum blocks stacked vertically with isolator frames in between. The thyatron was replaced with the solid state switch and the klystron modulator worked fine, so that the fluctuations of the RF power and its phase of the klystron output were reduced to 0.15 % and 0.1 degrees, respectively, both of which are one order of magnitude smaller than those using the thyatron.¹⁷ As a result, the fluctuation of the electron beam intensity decreased and that of the FEL beam intensity was significantly reduced accordingly.

After achieving high-intensity and stable operation of the FEL, we pursued further improvements in the FEL intensity. A straightforward method is to increase the electron beam intensity, or bunch charge. The output current of the electron gun in the FEL mode was 0.6 A, but the maximum emission current of the thermionic cathode (EIMAC YU-156) used in the electron gun is 18 A. The beam loading in the acceleration tube was so high that only a small portion of the input RF power remained at the RF output port, and therefore the electron gun current could not be increased any further. We have therefore developed a new method to increase bunch charge and to reduce the beam loading simultaneously. The electron bunch

intervals are 9.2 ns in the FEL mode, whereas the roundtrip time of light in the 5.531 m long cavity is 36.9 ns, which is four times longer than the bunch intervals, so that four FEL pulses reciprocate. One FEL pulse is sufficient for laser oscillation, and by extending the electron bunch intervals four times, the bunch charge can be quadrupled while keeping the beam loading constant. As a result, the micropulse energy may be quadrupled or even increased by the high current effect. We have developed a grid pulser for the electron gun in order to extend the electron bunch intervals four times. The grid pulser produces a square-wave pulse train with a width of 5 ns and a height of 150 V at intervals of 36.9 ns, or 27 MHz repetitions, for 8 μ s or more. The drive signal for the grid pulser is generated with the timing system of the linac and sent via an analog optical link to the pulser in the electron gun system, which is installed on the high voltage deck at 100kV DV in the tank pressured with SF₆ gas.¹⁸

By using the new grid pulser, the electron gun generated a series of electron pulses at intervals 36.9 ns with a peak current of 2.4 A, which is four times higher than that of the conventional one. The electron bunch charge in the accelerated electron beam was measured at the beam dumper of the FEL beamline to be 4 nC, which is four times higher than that in the conventional 108MHz mode, but the average current and accordingly the beam loading did not change at all. The maximum macropulse energy measured in the new mode, called the 27 MHz mode, reached 28.5 mJ at a wavelength of 65 μ m or a frequency of 4.6 THz. The macropulse energy obtained in the 108 MHz mode was 13 mJ in the same conditions except for the grid pulser.¹⁹ The macropulse energy in the 27 MHz mode is 2.2 times higher than that in the 108 MHz mode, but the micropulse energy in the 27 MHz mode increases by 8.7 times higher because the number of micropulses is a quarter of that in the 108 MHz mode.¹⁹

4. Characteristics of the 27 MHz mode

The energy of the electron beam accelerated by the L-band linac can be varied in the range from 12 to 19 MeV in the FEL mode,¹⁶ and the FEL beam can be generated in the wavelength range from 30 to 150 μ m,^{13, 14} or the frequency range from 10 down to 2 THz, depending on the wiggler gap and the electron energy. The electron energy is, however, currently fixed at 15 MeV for user experiments. Table 2 shows the characteristics of the electron beams and the FEL beams in two modes. Figure 2 shows the macropulse energy as a function of the peak wavelength measured by varying the wiggler gap. The wavelength is tunable from 40 to 110 μ m and the maximum energy is located at around 65 μ m. This measurement was performed with the detuning length of the optical cavity equal to zero, where the macropulse energy is the highest, the micropulse duration is the shortest, and the frequency width is the broadest. Figure 3 shows a temporal profile of the FEL macropulse measured with a high-speed pyroelectric detector at the electron energy of 15 MeV, wiggler gap of 37 mm, peak wavelength of around 70 μ m, and zero detuning length.

Table 2. Characteristics of the electron beams and the FEL beams in two modes.

Operation mode for FEL	27 MHz mode	108 MHz mode
Electron beam		
Electron beam energy (MeV)	15	15
Energy spread (FWHM, %)	1.2	1
Pulse length (μ s)	6	6
Bunch intervals (ns)	36.9	9.2
Number of electron bunches	160	650
Bunch charge (nC/bunch)	4	1
Bunch duration (ps)	20	20
Peak current in the bunch (A)	200	5
FEL beam		
Macropulse		
Maximum energy (mJ)	28.5	13
Peak wavelength (μ m)	65	70
Width (FWHM, μ s)	4	4
Micropulse		
Intervals (ns)	36.9	9.2
Number of micropulses	110	440
Maximum energy (μ J)	260	30

The inset is an expansion of the time axis around 6 μs , showing that the FEL micropulse intervals are 36.9 ns. The maximum micropulse energy can be evaluated, from the macropulse energy shown in Fig. 2 and the macropulse waveform in Fig. 3, to be 260 μJ , which is 24 times higher than that obtained in the first saturated operation of the FEL and nine times higher than that recently obtained in the 108 MHz mode.¹⁹

The detailed characteristics of the FEL are estimated using the maximum micropulse energy of 260 μJ measured at 65 μm or 4.6 THz in the 27 MHz mode. The micropulse width is estimated to be 2 ps, which was measured by the electro-optic sampling using a Ti-sapphire laser with a 100 fs duration that is synchronized to the 27 MHz clock signal of the linac timing system. The peak power of the micropulse is calculated to be 130 MW. The FEL beam taken out through a diamond window with diameter 20 mm into the air is an almost-parallel Gaussian beam with a standard deviation of 1.53 mm or a diameter of 3.6 mm (FWHM), so that the peak power density is calculated to be 0.88 GW/cm^2 . It can be focused with an off-axis parabolic mirror with a focal length of 12.5 mm and a diameter of 12.5 mm, so that the focusing angle is $\sigma' = 0.122$ rad for the parallel beam. The beam size of the diffraction limited radiation is calculated using the equation $\sigma \times \sigma' \cong \lambda/4\pi$ to be $\sigma = 42$ μm at the wavelength of 65 μm and the area of the focusing point is given by $S = 2\pi\sigma^2 = 1.13 \times 10^{-4}$ cm^2 . The peak power divided by the area yields the peak power density $I = 1.15$ TW/cm^2 . The electric field and the magnetic field of the THz beam at the focal point are calculated as $E = 2.9$ GV/m and $B = 9.8$ T, respectively, and these values are very large for a laser in the THz region. A sample application of a high electric field such as this is higher-order harmonic generation using a short-pulse high-intensity laser in the near-infrared region. According to an analysis of such experiments, the cutoff energy of the higher harmonic radiation E_{max} is approximately given by $E_{\text{max}} \sim I_p + 3U_p$, where I_p is the ionization energy of atoms, molecules, or ions and $U_p = e^2E^2/4m\omega^2$ is the ponderomotive energy with e the electron charge and m its mass, E the electric field, and $\omega = 2\pi c/\lambda$ the angular frequency of the THz wave, where λ is the wavelength and c is the speed of light.²⁰ Using the electric field of the focused THz FEL beam, the acceleration energy of an electron and the cutoff energy of the higher harmonics are calculated approximately to be 454 eV and 1.4 keV, respectively, which indicates possibilities for the use of the high electric and the magnetic fields produced by the THz FEL beam for material modifications.

5. Applications

The number of ISIR-FEL experiments has been gradually increasing. In this section several studies are

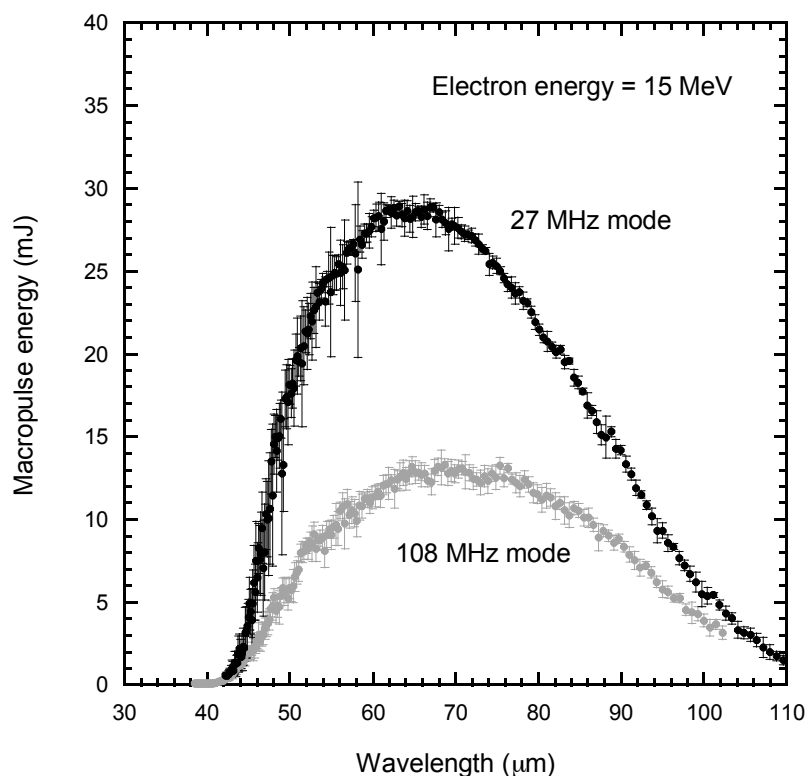


Fig. 2. Macropulse energies of FEL beams in the new 27 MHz mode as well as in the conventional 108 MHz mode measured with an energy meter at an electron energy of 15 MeV as a function of the magnet gap of the wiggler from 30 to 50 mm. See Table 2 for details.

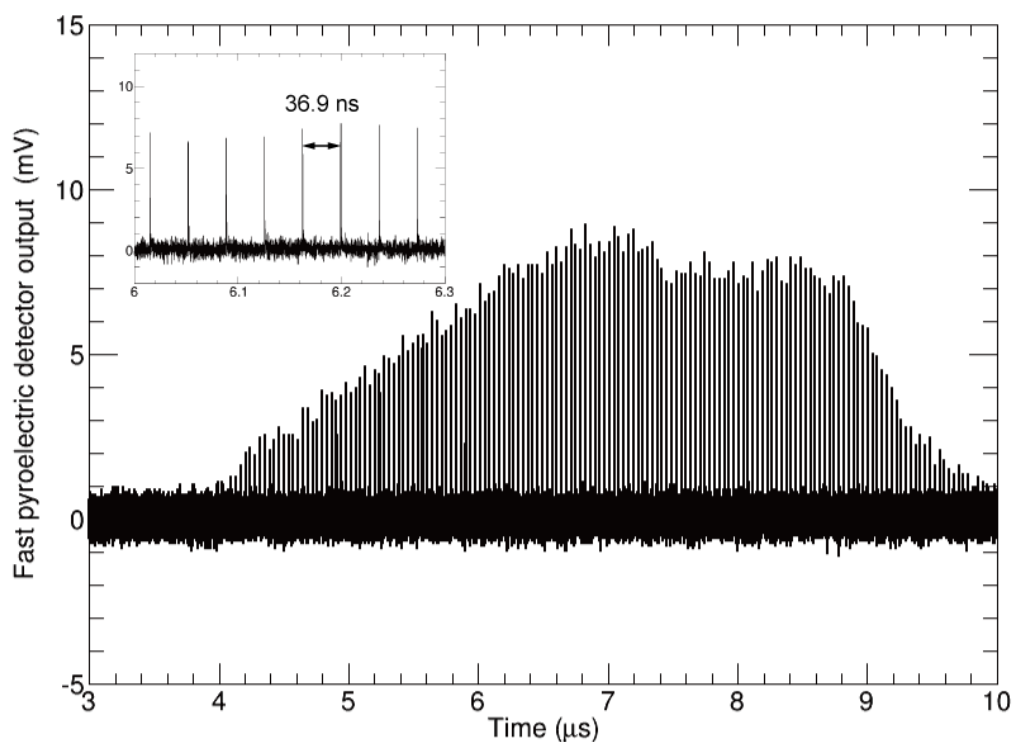


Fig. 3. FEL macropulse profile in the 27 MHz mode measured with a fast pyroelectric detector. An FEL macropulse consists of a series of FEL micropulses separated by 36.9 ns, which is equal to the electron bunch intervals in the 27 MHz mode listed in Table 2, as can be seen in the inset, which is an expansion of the time scale around 6.15 μ s. The full width at half maximum of the macropulse is approximately 4 μ s, which is used to estimate the number of micropulses and to calculate the mean micropulse energy using the measured macropulse energy.

briefly described. The first three studies are experiments in the liquid phase and the remaining three are in the solid phase.

- Polymer morphology change induced by terahertz irradiation²¹

The formation of micrometer-sized crystals was observed in a polymer (PHB)/chloroform solution irradiated by the THz beam. This demonstrated for first time that the THz wave effectively induces the intermolecular rearrangement of polymer macromolecules.

- Propagation of THz irradiation energy through aqueous layers: Demolition of actin filaments in living cells²²

The energy of THz pulses penetrates a millimeter deep, possibly as a shock wave, in aqueous solution and destroys actin filaments, even in the living cells. THz wave potentially alters protein structures in the living cells.

- Plane photoacoustic wave generation in liquid water using irradiation of terahertz pulses²³

The excitation of a large-area water surface irradiated by loosely focused THz light produces a plane photoacoustic wave owing to the strong absorption in water, and the plane wave propagates several millimeters, or 600 times the penetration depth of THz light in water, shorter than 10 μ m, which is observed by shadowgraph imaging. This method offers great advantages to non-invasive operations for industrial and biological applications.

- Luminescence induced by electrons outside zinc oxide nanoparticles driven by intense terahertz pulse trains²⁴

Nanoparticles of ZnO irradiated with an intense THz FEL emit luminescence not only from the nanoparticles but also from nitrogen molecules in the air, which shows a strong dependence on excitation frequency and a dependence on time in the macropulse. Field emitted electrons are effectively accelerated by the THz radiation and react with the nanoparticles to induce luminescence, which is a new excitation path of the nanoparticles.

- Significant volume expansion as a precursor to ablation and micropattern formation in phase change material induced by intense terahertz pulses²⁵

The phase change memory material $\text{Ge}_2\text{Sb}_2\text{Te}_5$ irradiated by intense THz pulse trains shows surface changes due to damage as a precursor to ablation and the formation of fine surface undulations with spatial period comparable to the wavelength of THz pulses or shorter. These changes are due not to thermal effects but to THz-induced ones, and they are important for laser material processing.

- Reconfiguration of magnetic domain structures of ErFeO_3 by intense terahertz free electron laser pulses²⁶

The shape of the ferromagnetic domain of a single ErFeO_3 crystal can be locally reconfigured by irradiating intense THz-FEL pulses near the domain boundary. Its mechanism can be phenomenologically understood by the combination of the depinning effect and the entropic force due to a local thermal gradient exerted by terahertz irradiation. Our finding opens up a new possibility of realizing thermal-spin effects in the THz frequency range by using THz-FEL pulses.

6. Summary

The THz FEL and the L-band linac have been progressively upgraded for higher intensity and stability. They cover the spectral range of 30 to 150 μm or from 2 to 10 THz, where absorption of water vapor is strong. The maximum micropulse energy reaches 260 μJ around a wavelength of 65 μm or a frequency of 4.6 THz, which is more than 10 times higher than other FELs in the wavelength region around 65 μm , by making the bunch charge four times higher. The estimated electromagnetic field of the focused FEL beam is $E = 2.9 \text{ GV/m}$ and $B = 9.8 \text{ T}$ at the wavelength and a free electron can be accelerated to 454 eV, though the photon energy at 4.6 THz is 19 meV only. The high-intensity narrow-band THz radiation can excite interatomic and intermolecular vibrational modes of solid and liquid materials and may change their structures to new ones that cannot be reached by other methods.

Acknowledgments

The author would like to thank all the people involved in this research for their various contributions to the development and utilization of the THz-FEL, including the coauthors of the papers in references 14, 16-19, and 21-26.

7. References

1. H.J. Eichler, J. Eichler, O. Lux, "Lasers: Basics, Advances and Applications", Springer Science in Optical Sciences, Vol. 220, Springer International Publishing, 2018, DOI: 10.1007/978-3-319-99895-4
2. D.A.G. Deacon, L.R. Elias, J.M.J. Madey, G.J. Ramian, H.A. Schwettman, T.I. Smith, First operation of a free-electron laser, *Phys. Rev. Lett.* 38 (1977) 892 – 894. doi.org/10.1103/PhysRevLett.38.892
3. S.V. Benson, J.M.J. Madey, J. Schultz, M. Marc, W. Wadensweiler, G.A. Westenskow, M. Velghe, The Stanford Mark III infrared free electron laser, *Nucl. Instr. Meth. A* 250 (1986) 39 -43. doi.org/10.1016/0168-9002(86)90857-0

4. H. Hama, J. Yamazaki and G. Isoyama, FEL Experiment on the UVSOR Storage Ring, *Nucl. Instr. Meth. A* 341 (1994) 12-6. doi.org/10.1016/0168-9002(94)90307-7
5. E.A. Seddon, J.A. Clarke, D.J. Dunning, C. Masciovecchio, C.J. Milne, F. Parmigiani, D. Rugg, J.C.H. Spence, N.R. Thompson, K. Ueda, S.M. Vinko, J.S. Wark and W. Wurth, Short-wavelength free-electron laser sources and science: a review, *Rep. Prog. Phys.* 80 (2017) 115901. doi.org/10.1088/1361-6633/aa7cca
6. G.R. Neil, S. Benson, G. Biallas, C.L. Bohn, D. Douglas, H.F. Dylla, R. Evans, J. Fugitt, J. Gubeli, R. Hill, K. Jordan, G. Krfft, R. Li, L. Merminga, D. Oepts, P. Piot, J. Preble, M. Shinn, T. Siggins, R. Walker, B. Yunn, First operation of an FEL in same-cell energy recovery mode, *Nucl. Instr. Meth. A* 445 (2000) 192 – 196. doi.org/10.1016/S0168-9002(00)00064-4
7. G. Ramian, The new UCSB free-electron lasers, *Nucl. Instr. and Meth. A* 318 (1992) 225 – 229. doi.org/10.1016/0168-9002(92)91056-F
8. J.M. Ortega, F. Glotin, R. Prazeres, Extension in far-infrared of the CLIO free-electron laser, *Infrared Phy. Technol.* 49 (2006) 133 – 138. doi.org/10.1016/j.infrared.2006.01.011
9. D. Oepts, A.F.G. van der Meer, P.W. van Amersfoort, The free-electron-laser user facility FELIX, *Infrared Phy. Technol.* 36 (1995) 297 – 308. doi.org/10.1016/1350-4495(94)00074-U
10. Y.U. Jeong, et al., First lasing of the KAERI compact far-infrared free-electron laser driven by a magnetron-based microtron, *Nucl. Instr. and Meth. A* 475 (2001) 47–50. doi.org/10.1016/S0168-9002(01)01533-9
11. E.A. Antokhin, et al., First lasing at the high-power free electron laser at Siberian center for photochemistry research, *Nucl. Instr. and Meth. A* 528 (2004) 15 – 18. doi.org/10.1016/j.nima.2004.04.009
12. U. Lehnert, et al., First experiences with the FIR-FEL at ELBE, *Proc. FEL 2007, Novosibirsk, Russia, 2007*, pp. 97 – 100. <http://accelconf.web.cern.ch/AccelConf/f07/PAPERS/proceedings.pdf>
13. S. Okuda, Y. Honda, N. Kimura, J. Ohkuma, T. Yamamoto, S. Suemine, T. Okada, S. Ishida, T. Yamamoto, S. Takeda, K. Tsumori, T. Hori, Free-electron laser oscillation with a multibunch electron beam of the 38 MeV L-band linear accelerator at ISIR, *Nucl. Instrum. Meth. A* 358 (1995), 244. doi.org/10.1016/0168-9002(94)01592-9
14. R. Kato, S. Kondo, T. Igo, T. Okita, T. Konishi, S. Suemine, S. Okuda, G. Isoyama, Lasing at 150 μm wavelength and measurement of characteristics of the free-electron laser at ISIR, Osaka University, *Nucl. Instrum. Meth. A* 445 (2000) 169 – 172. doi.org/10.1016/S0168-9002(00)00057-7
15. G. Dattoli and A. Renieri : in *Laser Handbook Vol. 4*, eds. M.L. Stitch and M. Bass (North-Holland, Amsterdam, 1985).
16. K. Kawase, Y. Morio, Y. Kon, M. Fujimoto, S. Hirata, J. Shen, R. Kato, A. Irizawa, G. Isoyama, S. Kashiwagi, Feed-forward control of the amplitude and the phase of a high-power RF pulse based on the overdrive technique, *Nucl. Instr. Meth. A* 679 (2012) 44-53. doi.org/10.1016/j.nima.2012.03.004
17. A. Tokuchi, F. Kamitsukasa, K. Furukawa, K. Kawase, R. Kato, A. Irizawa, M. Fujimoto, H. Osumi, S. Funakoshi, R. Tsutsumi, S. Suemine, Y. Honda, Goro Isoyama, Development of a high-power solid-state switch using static induction thyristors for a klystron modulator, *Nucl. Instr. Meth. A* 769 (2015) 72-78 doi.org/10.1016/j.nima.2014.09.063
18. S. Suemine, K. Kawase, N. Sugimoto, S. Kashiwagi, K. Furukawa, R. Kato, A. Irizawa, M. Fujimoto, H. Osumi, M. Yaguchi, S. Funakoshi, R. Tsutsumi, K. Kubo, A. Tokuchi, G. Isoyama, Grid pulser for an electron gun with a thermionic cathode for the high-power operation of a terahertz free-electron laser, *Nucl. Instr. Meth. A* 773 (2015) 97-103. doi.org/10.1016/j.nima.2014.10.071

19. K. Kawase, M. Nagai, K. Furukawa, M. Fujimoto, R.Kato, Y. Honda, G. Isoyama, Extremely high-intensity operation of a THz free-electron laser using an electron beam with a higher bunch charge, *Nucl. Instr. Meth. A*960 (2020) 163582-1~5. doi.org/10.1016/j.nima.2020.163582
20. J.L. Krause, K.J. Schafer, C.K. Kulander, High-order harmonic generation from atoms and ions in the high intensity regime, *Phys. Rev. Lett.* 68 (1992) 3535 – 3538. doi.org/10.1103/PhysRevLett.68.3535
21. H. Hoshina, H. Suzuki, C. Otani, M. Nagai, K. Kawase, A. Irizawa and G. Isoyama, Polymer morphological change induced by terahertz irradiation, *Sci. Rep.* 6 (2016) 27180-1~6. doi.org/10.1038/srep27180
22. S. Yamazaki, M. Harata, Y. Ueno, M. Tsubouchi, K. Konagaya, Y. Ogawa, G. Isoyama, C. Otani, H. Hoshina, Propagation of THz irradiation energy through aqueous layers: Demolition of actin filaments in living cells, *Sci. Rep.* 10, 9008 (2020) 1~10. doi.org/10.1038/s41598-020-65955-5
23. M. Tsubouchi, H. Hoshina, M. Nagai, and G. Isoyama, Plane photoacoustic wave generation in liquid water using irradiation of terahertz pulses, *Sci. Rep.* 10, 18537 (2020) 1~9. doi.org/10.1038/s41598-020-75337-6
24. M. Nagai, S. Aono, M. Ashida, K. Kawase, A. Irizawa and G. Isoyama, Luminescence induced by electrons outside zinc oxide nanoparticles driven by intense terahertz pulse trains, *New J. Phys.* 19 (2017) 053017-1~9, doi.org/10.1088/1367-2630/aa6e19
25. K. Makino, K. Kato, K. Takano, Y. Saito, J. Tominaga, T. Nakano, G. Isoyama, and M. Nakajima, Significant volume expansion as a precursor to ablation and micropattern formation in phase change material induced by intense terahertz pulses, *Sci. Rep.* 8, 2914-1-8 (2018). doi.org/10.1038/s41598-018-21275-3
26. T. Kurihara, K. Hirota, H. Qiu, K. T. N. Phan, K. Kato, G. Isoyama & M. Nakajima, Reconfiguration of magnetic domain structures of ErFeO₃ by intense terahertz free electron laser pulses, *Sci. Rep.* 10, 7321 (2020) 1~6 doi.org/10.1038/s41598-020-64147-5